

High Galactic latitude *Fermi* sources of γ -rays with energies above 100 GeV

A. Neronov¹, D. Semikoz^{2,3}, and Ie. Vovk¹

¹ ISDC Data Centre for Astrophysics, Ch. d'Ecogia 16, 1290 Versoix, Switzerland
e-mail: Andrii.Neronov@unige.ch

² APC, 10 rue Alice Domon et Léonie Duquet, 75205 Paris Cedex 13, France
e-mail: dmitri.semikoz@apc.univ-paris7.fr

³ Institute for Nuclear Research RAS, 60th October Anniversary prosp. 7a, Moscow 117312, Russia

Received 4 August 2010 / Accepted 6 February 2011

ABSTRACT

Aims. We present a catalog of sources of very high energy ($E > 100$ GeV) γ -rays detected by the Large Area Telescope (LAT) onboard the *Fermi* Gamma-Ray Space Telescope at Galactic latitudes $|b| \geq 10^\circ$.

Methods. We cross-correlate the directions of individual photons with energies above 100 GeV detected by *Fermi* /LAT with the first year *Fermi* catalog of sources detected at lower energies. We find a significant correlation between the arrival directions of the highest energy photons and positions of *Fermi* sources, with the possibility of chance coincidences at the level of 10^{-45} . We present a list of *Fermi* sources contributing to the correlation signal. A similar analysis is performed to cross-correlate the catalog of BL Lac objects with the highest energy photons detected by *Fermi*.

Results. We produce a catalog of high Galactic latitude *Fermi* sources visible at 100–300 GeV energies. The catalog is divided into two parts. The first part contains a list of 50 higher significance sources among which there can be three possible false detections. The second part of the catalog contains a list of 25 lower significance sources, among which six are possibly false detections. Finally we identify eight additional sources from the cross-correlation analysis with the BL Lac catalog. The reported sources of $E > 100$ GeV γ -rays span a broad range of redshifts, up to $z \sim 1$. Most of the sources are BL Lac type objects. Only 17 out of 83 objects in our list were previously reported as VHE γ -ray sources.

Key words. gamma rays: galaxies – galaxies: active – surveys

1. Introduction

Ground-based Cherenkov γ -ray telescopes HESS, MAGIC, and VERITAS have discovered a population of sources of very high energy (VHE) ($E \geq 100$ GeV) γ -rays. Except for the sources discovered in the Galactic plane survey by HESS (Aharonian et al. 2005, 2006), most of the sources were discovered in dedicated pointed observations. Surveys of large regions of the VHE γ -ray sky with the existing Cherenkov telescopes are difficult because of the too-narrow size of the field of view. The wide field-of-view ground-based γ -ray detectors MILAGRO (Atkins et al. 2004) and Tibet (Amenomori et al. 2005) arrays have produced a systematic survey of the VHE γ -ray sky. The energy threshold of the air shower arrays such as MILAGRO and Tibet is rather high (in the multi-TeV band) so that only sources with spectra extending well above 1 TeV could be detected.

All-sky monitoring of γ -ray sources at the energies $E \sim 100$ GeV became possible with the start of operation of the Large Area Telescope (LAT) onboard the *Fermi* Gamma-Ray Space Telescope. Compared to the ground-based γ -ray telescopes, the LAT has a much smaller effective area (~ 1 m², compared to $\sim 10^5$ m² for the ground-based γ -ray telescopes). At the same time, at the energies above 100 GeV the *Fermi* signal is almost background-free (in contrast to the ground based telescopes in which the signal has to be identified on top of the strong background created by cosmic rays and optical/UV night sky background). Neronov et al. (2010) searched for the point sources of $E \geq 100$ GeV γ -rays using *Fermi* data and found eight

significant excesses with at least three photons within a 0.1° circle corresponding to the 68% containment radius of the point spread function (PSF) of the LAT. Seven excesses were associated with known VHE γ -ray sources, while the remaining one was identified with the head-tail radio galaxy IC 310. Detection of IC 310 in the VHE band was later confirmed by the MAGIC telescope (Mariotti 2010). Owing to the moderate collection area of *Fermi*, only the brightest VHE γ -ray sources were detected individually in the *Fermi* VHE γ -ray sky survey. All other known VHE γ -ray sources at Galactic latitudes $|b| \geq 10^\circ$ gave ≤ 2 photons within the LAT PSF circle and could not be found from the analysis of the data above 100 GeV alone.

A complementary method for identifying the sources of $E \geq 100$ GeV photons detected by *Fermi* is to use prior knowledge of source positions on the sky and to verify which of the already known sources could have produced the highest energy γ -rays detected by the LAT telescope. In other words, sources of $E \geq 100$ GeV γ -rays could be identified also via cross-correlation of arrival directions of the $E \geq 100$ GeV γ -rays with the source positions on the sky. This approach to the identification of the sources was previously applied to the analysis of EGRET data above 10 GeV by Dingus & Bretsch (2001) and Gorbunov et al. (2005).

We perform the cross-correlation analysis of the arrival directions of γ -rays with energies above 100 GeV detected by *Fermi* at Galactic latitudes $|b| \geq 10^\circ$ with the first year *Fermi* source catalog (Abdo et al. 2010a). Our analysis results in a catalog of 50 high Galactic latitude sources that correlate with the

arrival directions of $100 \text{ GeV} \leq E \leq 300 \text{ GeV}$ γ -rays within a 68% containment circle of LAT PSF. Among these 50 sources, seven sources that correlate with ≥ 3 VHE γ -rays (considered previously by [Neronov et al. 2010](#)) are detected above 100 GeV with significance $\geq 8\sigma$. Six sources that correlate with two photons are detected with a significance of around $4\text{--}5\sigma$. Each individual source that correlates with just one VHE γ -ray has a significance of around 3σ in this energy band, the overall significance of the detection of the entire source set being very high. The chance coincidence probability of $E > 100 \text{ GeV}$ γ -ray arrival directions correlating with the source positions is $< 10^{-40}$ (excluding the seven high significance sources from [Neronov et al. 2010](#)), which corresponds to the significance of detection of the entire set of $50 - 7 = 43$ sources $> 13\sigma$. The sources correlating with only one $E > 100 \text{ GeV}$ photon should be considered as “VHE source candidates”. A simple analysis indicates that most of the sources contributing to the correlation signal are real VHE γ -ray sources, only three of them being expected to be false detections. Taking into account that most of the sources in the list are BL Lac type objects, we extend our cross-correlation analysis to the catalog of BL Lacs ([Veron-Cetty & Veron 2010](#)) and find eight more sources that correlate with the arrival directions of $100 \text{ GeV} \leq E \leq 300 \text{ GeV}$ γ -rays and are not listed in the first year *Fermi* catalog. For completeness, we list sources from the first year *Fermi* catalog for which the $E \geq 100 \text{ GeV}$ γ -rays are found within a circle of the radius at which the correlation signal is strongest. Its radius is somewhat larger than the 68% containment circle of LAT PSF. There are 25 such sources, six of them being expected to be false detections because of the chance coincidence of the arrival direction of the VHE γ -ray with the source position. For energies $E > 300 \text{ GeV}$, we found correlations with four known sources, one possible new source and one false detection.

The plan of the paper is as follows. In Sect. 2 we discuss data selection and data analysis methods. In Sect. 3, we present the results of the correlation analysis of the arrival directions of $E \geq 100 \text{ GeV}$ γ -rays with the sources of the first year *Fermi* catalog. In Sect. 4, we provide the list of sources contributing to the correlation signal. In Sect. 5 we perform the correlation analysis with the BL Lac catalog of [Veron-Cetty & Veron \(2010\)](#) and give the list of additional BL Lacs correlating with the highest energy *Fermi* photons, but not present in the first year *Fermi* catalog. In Sect. 6 we discuss correlations of $E \geq 300 \text{ GeV}$ photons with all possible sources discussed above. In Sect. 7 we comment upon individual sources. Finally, in Sect. 8 we discuss the results.

2. Data selection and data analysis

For our analysis, we used the LAT data collected in the period between August 4, 2008 and June 25, 2010. The data were filtered using the *gtselect* tool provided by Fermi Science Tools¹, so that only γ -ray events ($\text{evc1s}=3$) with energies above 100 GeV were retained in the analysis. The resulting list of photons has 6376 events. A fraction of the $E \geq 100 \text{ GeV}$ photons comes from directions close to the Galactic plane, which is a source of significant diffuse γ -ray emission even at photon energies higher than 100 GeV. Presence of strong diffuse emission complicates the analysis of the point source contribution. Taking this into account, we consider only photons coming from Galactic latitudes $|b| \geq 10^\circ$. The cut on the Galactic latitude leaves 4086 photons for the analysis.

For energies $E < 300 \text{ GeV}$, photons are thought to be clearly distinguishable from cosmic rays in *Fermi*, while at $E > 300 \text{ GeV}$ ($\text{evc1s}=3$) the sample contains an unknown number of misidentified cosmic rays ([Atwood et al. 2009](#)). We therefore divide data into two energy bins divided at $E = 300 \text{ GeV}$. There are 3186 photons with energies $100 \text{ GeV} \leq E \leq 300 \text{ GeV}$, for which we perform our main analysis in the following sections, and there are in addition 900 photons with energies $E > 300 \text{ GeV}$, which we discuss separately in Sect. 6².

The set of photons considered in the analysis includes the list of photons studied by [Neronov et al. \(2010\)](#). In our analysis, we exclude the high-confidence sources of VHE γ -rays identified by [Neronov et al. \(2010\)](#). We also exclude 75 γ -ray photons associated with these eight sources from the *Fermi* $E \geq 100 \text{ GeV}$ photon list, i.e. found within 0.2 degrees of those sources. Otherwise, these sources would dominate the correlation signal. Nevertheless, we include the high-confidence sources in the final source list given in the Table 1, to obtain a complete catalog of sources of VHE γ -rays found by *Fermi*. The final photon list used in the analysis includes 3111 photons with $|b| \geq 10^\circ$.

Photons detected by *Fermi*/LAT are divided into two types – *front-* and *back-*converting. Photons that pair-convert in the top 12 layers of the tracker are classified as front-converting, and are otherwise back-converting ([Abdo et al. 2010b](#)). At the same energy, front-converting photons have a somewhat sharper PSF³. We take this into account by considering the sets of 1179 front- and 1934 back-converted photons separately in our correlation analysis.

If the sky region around the source is not too crowded, the point spread functions of individual *Fermi* sources do not overlap at the energies above $\sim 1 \text{ GeV}$. At high Galactic latitudes, the strength and complexity of the diffuse Galactic γ -ray background at energies above 1 GeV is far lower than the low-latitude/low-energy background. We calculate the spectra of the sources using two methods, one the unbinned likelihood analysis performed using the *gtlike* tool in narrow energy bins (see http://fermi.gsfc.nasa.gov/ssc/data/analysis/scitools/likelihood_tutorial.html) and the other using the aperture photometry method for the same energy bins. In each case, we verify that the two analysis methods provide consistent results. The aperture photometry method is most useful at the highest energies, at which the photon statistics is low. In this method, we first calculate for each source and each energy the number of source counts within a circle of the radius equal to the 95% containment circle of the LAT PSF and calculate the LAT exposure within this circle using the *gtexposure* tool. The errors in the measurements are calculated based on a Poisson distribution, which provides the correct description of the data at low photon statistics. To estimate the diffuse sky background at the position of the source, we calculate the number of background counts in a ring with the outer radius 3° and the inner radius equal to the 95% containment radius of the LAT PSF, centered on the source. We verified that the results obtained using such an intuitively simple spectral extraction procedure are consistent with those obtained via spectral extraction using likelihood

² For the method discussed below, it does not matter whether the background consists of photons or misidentified cosmic rays. We are grateful to I.Tkachev and P.Tinyakov, who pointed out that we can use photons with $E > 300 \text{ GeV}$ in our analysis.

³ http://www-glast.slac.stanford.edu/software/IS/glast_lat_performance.htm

¹ <http://fermi.gsfc.nasa.gov/ssc/data/analysis/>

Table 1. List of *Fermi* sources for which a 100 GeV $\leq E \leq 300$ GeV photon is found within the 68% containment circle of radius 0.1°.

	1FGL	RA	Dec	N_{68}	P_{68}	N_{68}	N_{min}	P	TS	Type ¹	Name	z
				30–100	30–100	100–300	[N_{95}]	100–300				
1	J0033.5-1921	8.3913	-19.3650	6	2.1×10^{-14}	1b	1	2.3×10^{-5}	21	BL V	RBS 76	0.61
2	J0054.9-2455	13.7337	-24.9290	0	–	1f		3.2×10^{-3}	18			
3	J0110.0-4023	17.5250	-40.3887	1	1.3×10^{-2}	1f		2.4×10^{-3}	12			
4	J0209.3-5229	32.3392	-52.4907	2	1.1×10^{-4}	1f		3.5×10^{-3}	12	BL Vf	RBS 285	
5	J0213.2+2244	33.3225	22.7489	2	1.6×10^{-4}	1b		2.6×10^{-3}	13	QSO	1RXS J021252.2+22	
6	J0222.6+4302	35.6681	43.0385	16	4.6×10^{-40}	3f1b	1	1.4×10^{-13}	75	BL V	3C 66A	0.444
7	J0237.5-3603	39.3788	-36.0530	3	2.3×10^{-7}	1b		2.4×10^{-3}	15	BL V	RBS 334	
8	J0303.5-2406	45.8890	-24.1124	9	2.0×10^{-23}	2f	[1]	1.8×10^{-6}	39	BL Vf	<u>PKS 0301-243</u>	0.26
9	J0315.9-2609	48.9933	-26.1581	1	1.4×10^{-2}	2b		3.5×10^{-6}	28	BL V	<u>RX J0316.2-2607</u>	0.443
10	J0316.3-6438	49.0996	-64.6411	0	–	1b		1.5×10^{-3}	13			
11	J0322.1+2336	50.5396	23.6108	2	2.0×10^{-4}	1f		4×10^{-3}	16	BL Vf	RGB J0321+236	
12	J0325.9-1649	51.4780	-16.8174	0	–	1b		2.5×10^{-3}	12	BL V	RBS 421	0.29
13	J0338.8+1313	54.7212	13.2314	0	–	1b		3.1×10^{-3}	13			
14	J0416.8+0107	64.2069	1.1244	0	–	1f		2.5×10^{-3}	14	BL Vf	2E 0414+0057	
15	J0428.6-3756	67.1567	-37.9412	9	3.4×10^{-22}	1f		2.9×10^{-3}	18	BL	PKS 0426-380	1.11
16	J0505.9+6121	76.4853	61.3527	1	1.9×10^{-2}	1f	[2]	1.6×10^{-6}	21			
17	J0507.9+6738	76.9931	67.6367	12	2.7×10^{-29}	2f2b	3	3.8×10^{-19}	96	BL V	1ES 0502+675	0.341
18	J0543.8-5531	85.9512	-55.5301	1	2.0×10^{-2}	1f1b		5.3×10^{-6}	34	BL V	<u>RBS 679</u>	
19	J0650.7+2503	102.6817	25.0622	1	1.0×10^{-2}	1f		2.2×10^{-3}	15	BL V	1ES 0647+250	0.203
20	J0710.6+5911	107.6595	59.1853	3	2.3×10^{-6}	1f		2.0×10^{-3}	17	BL	RX J0710.4+5908	0.125
21	J0721.9+7120	110.4794	71.3448	9	6.3×10^{-21}	1f		3.6×10^{-3}	13	BL Vf	S5 0716+71	0.3
22	J0745.2+7438	116.3215	74.6415	0	–	1b		3.9×10^{-3}	10	BL V	1ES 0737+746	0.315
23	J0809.4+3455	122.3539	34.9331	0	–	1f		2.5×10^{-3}	14	BL Vf	B2 0806+35	0.0825
24	J0809.5+5219	122.3856	52.3178	5	3.1×10^{-11}	1f1b		5.9×10^{-6}	25	BL Vf	1ES 0806+524	0.138
25	J0816.4-1311	124.1121	-13.1933	5	5.5×10^{-13}	1f		1.8×10^{-3}	13	BL Vf	PMN J0816-1311	
26	J0905.5+1356	136.3916	13.9483	1	1.5×10^{-2}	1b		4.0×10^{-3}	14	QSO?	SDSS J090513.28 +140240.3	1.12
27	J0915.7+2931	138.9412	29.5319	3	8.6×10^{-7}	1f		2.7×10^{-3}	13	BL Vf	B2 0912+29	
28	J0953.0-0838	148.2673	-8.6461	2	9.5×10^{-5}	1f		2.6×10^{-3}	15	BL Vf	PMN J0953-840	
29	J0957.7+5523	149.4315	55.3922	6	2.1×10^{-13}	1b		3.6×10^{-3}	12	QSO	4C +55.17	0.8955
30	J1015.1+4927	153.7885	49.4526	5	2.9×10^{-11}	1b	2	2.6×10^{-7}	35	BL V	1ES 1011+496	0.212
31	J1104.4+3812	166.1247	38.2108	57	0	14f8b	3[1]	0	494	BL V	<u>Mkn 421</u>	0.03
32	J1117.1+2013	169.2993	20.2222	3	5.5×10^{-7}	1f		2.9×10^{-3}	12	BL Vf	RBS 958	0.1
33	J1133.1+0033	173.2792	0.56306	0	–	1f		2.9×10^{-3}	11	BL V	PKS B1130+008	1.223
34	J1217.7+3007	184.4463	30.1206	2	2.0×10^{-4}	1b		3.0×10^{-3}	8	BL V	B2 1215+30	0.13
35	J1224.7+2121	186.1987	21.3633	6	7.3×10^{-14}	1f1b		1.7×10^{-6}	31	FSRQ	<u>4C +21.35</u>	0.432
36	J1309.5+4304	197.3933	43.0669	3	8.8×10^{-7}	1f		2.9×10^{-3}	13	BL Vf	B3 1307+433	0.69
37	J1337.7-1255	204.4336	-12.9289	0	–	1f		1.5×10^{-3}	15	FSRQ	PKS 1335-127	0.539
38	J1437.0+5640	219.2617	56.6720	4	5.7×10^{-9}	1f		3.4×10^{-3}	17	BL	RBS 1409	0.15
39	J1555.7+1111	238.9383	11.1921	25	0	3f2b	1[1]	3×10^{-16}	124	BL V	PG 1553+113	
40	J1653.9+3945	253.4897	39.7527	17	1.1×10^{-44}	9f1b	1	1.5×10^{-32}	214	BL V	<u>Mkn 501</u>	0.0336
41	J1722.5+1012	260.6494	10.2144	0	–	1f		2.3×10^{-3}	17	FSRQ	TXS 1720+102	
42	J1744.2+1934	266.0710	19.5706	1	2.1×10^{-2}	1b		2.5×10^{-3}	13	BL V	1ES 1741+196	0.083
43	J1824.6+1013	276.1739	10.2180	0	–	1f		1.9×10^{-3}	10			
44	J2000.0+6508	300.0215	65.1334	7	2.1×10^{-15}	1f	[1]	1.9×10^{-4}	20	BL Vf	1ES 1959+650	0.048
45	J2000.9-1749	300.2467	-17.8286	1	2.2×10^{-2}	1b		4.0×10^{-3}	11	FSRQ	PKS 1958-179	0.65
46	J2004.8+7004	301.2074	70.0710	0	–	1b		4.3×10^{-3}	13			
47	J2009.5-4849	302.3761	-48.8295	7	1.3×10^{-15}	4f1b	[1]	7.5×10^{-15}	82	BL V	PKS 2005-489	0.071
48	J2158.8-3013	329.7117	-30.2176	23	0	5f3b	1[1]	2.2×10^{-24}	164	BL V	PKS 2155-304	0.117
49	J2314.1+1444	348.5487	14.7463	1	1.8×10^{-2}	1f		3.1×10^{-3}	13	AGN	SDSS J231405.46 +143904.6	1.319
50	J2322.6+3435	350.6540	34.5839	1	2.0×10^{-2}	1f		3.4×10^{-3}	14	BL	TXS 2320+343	0.098

Notes. First column: *Fermi* source ID; 2nd column: Right Ascension; 3rd column: Declination; 4th column: number of photons in the 68% containment circle in 30–100 GeV band; 5th column: chance coincidence probability to find given number of photons in the 68% containment circle in 30–100 GeV band; 6th column: number of photons in the 68% containment circle in 100–300 GeV band; “f” marks front photons, “b” marks back photons; 7th column: number of photons in the $\theta \leq 0.17^\circ$ circle around the source or in the 95% containment circle of the radius 0.3° (square brackets); 8th column: chance probability to find given number of background photons within 0.1° and 0.17° [0.3°] circles around the source position; 9th column: TS value in 100–300 GeV energy bin, found with our analysis; 10th column: source type; 11th column: alternative name of the source; 12th column: source redshift. Bold marks the sources which have been previously detected in the VHE band by ground-based γ -ray telescopes. Underlined are sources detected with *Fermi* in 100–300 GeV band with $TS > 25$. The updated version of this table is available online at <http://www.isdc.unige.ch/vhe/>. ¹ BL – BL Lac type object; QSO – quasi-stellar object, AGN – active galactic nucleus, FSRQ – flat spectrum radio quasar; FR I – Fanaroff-Riley type I radio galaxy; V – also found from the correlation analysis with the BL Lac catalog; Vf – front photon contributes to the correlation signal with the BL Lac catalog.

analysis in narrow energy bins and/or likelihood analysis in the wide energy range using a specific broad-band spectral model.

3. Correlation between arrival directions of $E \geq 100$ GeV photons and sources from the first year *Fermi* catalog

To find sources of $E \geq 100$ GeV γ -rays that cannot individually be recognized in the *Fermi* data in this energy band, we apply a method similar to the one discussed by [Dingus & Bretsch \(2001\)](#) and [Gorbunov et al. \(2005\)](#). Using this method, sources producing just a few photons could be identified. A fraction of identified sources might be false detections because of a chance coincidence of the source position with the arrival direction of a background photon. The fraction of positive-to-false detections could be readily estimated. Real sources should largely outnumber the false source detections. This makes the list of sources contributing to the correlation a valuable “input catalog” for the observations with ground-based γ -ray telescopes that are more sensitive than *Fermi* in the VHE γ -ray band, but, in contrast to *Fermi*, do not have all-sky survey capabilities.

As a first choice, we took the first year *Fermi* catalog as an input catalog for the correlation analysis ([Abdo et al. 2010a](#)). The catalog contains 1451 sources, 1043 of which are objects with $|b| \geq 10$ degrees. Removing seven confirmed VHE γ -ray sources from the list of [Neronov et al. \(2010\)](#) (IC 310 is not in the *Fermi* catalog), we obtain an input catalog of $N_{\text{source}} = 1036$ sources.

The probability that a γ -ray photon originates within a given distance θ from one source in the catalog is estimated as the ratio of the area of the circle of radius θ to the part of the sky at $|b| \geq 10^\circ$

$$p_1 = \frac{\pi\theta^2}{4\pi(1 - \cos(80^\circ))} \simeq 9.2 \times 10^{-7} \left[\frac{\theta}{0.1^\circ} \right]^2. \quad (1)$$

The total probability of a photon originating within an angle θ of one of the catalog sources is then

$$p = N_{\text{source}} \cdot p_1 = 9.5 \times 10^{-4} \left[\frac{N_{\text{source}}}{1036} \right] \left[\frac{\theta}{0.1^\circ} \right]^2. \quad (2)$$

The probability that K or more photons from $N_\gamma = 3111$ γ -rays come within the angle θ from any of sources in the catalog by chance is given by the binomial probability

$$P(\theta) = \sum_{k=K}^{N_{\text{tot}}} p^k (1-p)^{N_\gamma-k} \frac{N_\gamma!}{(N_\gamma-k)!k!}. \quad (3)$$

In Fig. 1, we plot this probability as a function of angle θ . The probability that γ -rays with energies higher than 100 GeV come from directions close to the positions of *Fermi* sources by chance is $P < 10^{-45}$, i.e. the chance coincidence hypothesis is firmly ruled out.

The function $P(\theta)$ has two minima at around 0.1 degrees and 0.17 degrees. This is explained by how precision with which the arrival direction is determined for the front and back converted γ -rays differs. To verify this, we divide the whole photon list into two parts corresponding to the front and back converted γ -rays and plot the contributions of those photons separately. From Fig. 1, one can see that the minimum at 0.1 degree is due to front photons, while the minimum at 0.17 degrees is due to both front and back photons.

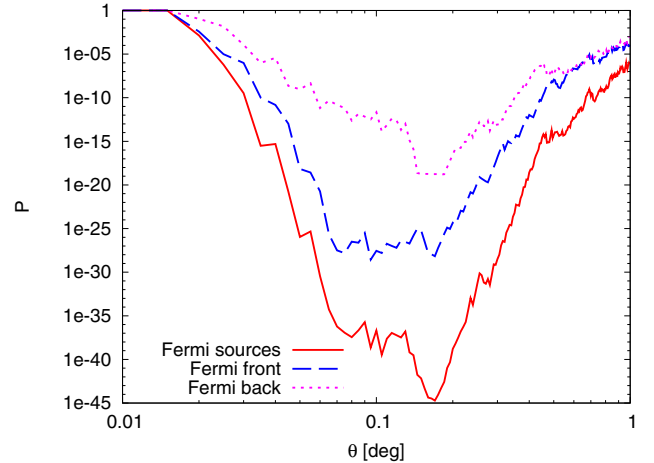


Fig. 1. Dependence on the chance probability of correlation between arrival directions of $E \geq 100$ GeV photons and positions of *Fermi* sources as a function of the radius of the search circle. Solid curve corresponds to all photons. Dashed and dotted curves correspond to, respectively, front- and back-converted photons.

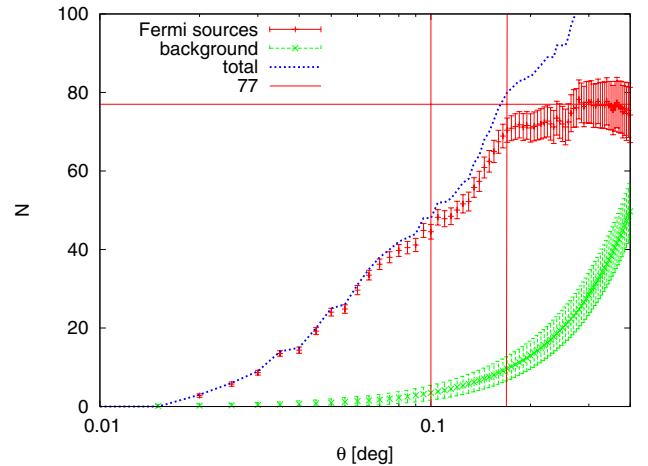


Fig. 2. Number of events that come from *Fermi* sources as a function of the radius of the search circle (red data points). Error bars indicate fluctuations in the background when determining the signal from the sources. Average number of background photons is shown with green line. Vertical line at 0.1 degree is the radius of the 68% containment circle of *Fermi* PSF. The vertical line at 0.17 degree shows the position of the dip in the probability shown in Fig. 1. The horizontal line indicates the asymptotic number of photons from all the sources.

In Fig. 2, we plot the number of source photons with arrival directions within the angle θ from the catalog of *Fermi* sources and compare it to the expected number of background events within the same distance from the sources. To estimate the number of background events, we used two alternative methods. First, we estimated the expected background near each source counting all photons within 10 degrees from it and estimating the fraction of photons that originate within the angle θ . This method can be used only for $\theta \lesssim 0.5^\circ$. For $\theta \gtrsim 0.5^\circ$, circles around the *Fermi* sources cover a significant fraction of the sky and overlap. In the second method, we estimated the background by generating 3111 photons in the sky outside the Galactic plane $|b| > 10^\circ$. We followed the *Fermi* exposure which had been estimated using the *gtexposure* tool by keeping Galactic b-values of events and generating randomly l -values. This takes into account

the remaining contribution of the Galaxy for $|b| > 10^\circ$. After that, we average over many Monte Carlo simulations. Both methods gave similar results for small angles.

Vertical lines in Fig. 2 show the angular positions of the two minima of probability seen in Fig. 1. The minima correspond to the places where the steep rise in the number of signal events changes to a plateau. The asymptote of the distribution of signal counts at large θ gives an estimate of the total number of γ -rays contributing to the correlation. One can see that only ~ 77 out of 3111 events come from known *Fermi* sources. 48 for these 77 events are displaced by less than 0.1° from the catalog source position. In this circle, one expects only $N_{B, 0.1} \approx 3$ background events. No more than seven background photons are expected at the 95% confidence level and no more than nine background photons are expected at the 99.5% confidence level. The number of events contributing to the correlation within $\theta = 0.17^\circ$ circle is $N_{S, 0.17} \approx 71$, while the expected number of background events is $N_{B, 0.17} \approx 7.7$ (13 at the 95% confidence level, 15 at the 99% confidence level).

4. Catalog of extragalactic VHE γ -ray sources

The list of sources contributing to the correlation signal within $\theta = 0.1^\circ$ is given in Table 1. There are $N_{\text{Source}, 0.1} = 50 - 7 = 43$ sources, if the sources from the list of Neronov et al. (2010) are excluded. For $N_\gamma = 3111$, only $p \cdot N_\gamma \approx 3$ photons on average can be at the distance $\theta \leq 0.1^\circ$ from a catalog source by chance. This means that 3 out of 43 new VHE γ -ray sources listed in Table 1 are expected to be false detections (and no more than 7[9] sources are false detections at the 95% [99.5%] confidence level).

It is not possible to know in advance which of the 43 sources from Table 1 are false detections. In principle, the ten sources that have more than one photon within the 95% containment circle of the LAT PSF are not expected to be false detections, because the probability that two background photons come close to one and the same source is much smaller than the same probability for just one background photon. Additional information that might help us to single out the false detections could be obtained by comparing of the estimate of the source fluxes expected from the extrapolation of the measured spectral characteristics of the sources in the 1–100 GeV energy band with the simple estimates of the flux that produces one photon at $E \geq 100$ GeV within 1.8 year exposure with *Fermi*. In principle, a false detection might be spotted if the source contributing to the correlation has low flux and/or a soft spectrum. This is illustrated in Fig. 3 where the distribution of fluxes and photon indices of the AGN from the *Fermi* AGN catalog (Abdo et al. 2010c) is compared to the distribution of fluxes and photon indices of the sources from Table 1. Dashed lines show the combinations of the spectral parameters that are expected to give a fixed number of photons in the 100–300 GeV band, assuming no high-energy cut-off in the spectrum.

Figure 4 shows the measurements of the source fluxes in 0.3–1 GeV, 1–3 GeV, 3–10 GeV, and 10–100 GeV for the entire 1.8 yr *Fermi*/LAT exposure in addition to the estimates of the source fluxes in the 100–300 GeV band based on the number of $E \geq 100$ GeV detected photons from each source.

Although the significance of the detection of individual sources of 1(2) photons in the 100–300 GeV band in Table 1 is around $3\sigma(4\sigma)$, some of the sources are detected with a significance higher than 5σ in the adjacent 30–100 GeV energy band. The 5th and 6th columns of Table 1 show the numbers of photons and the chance coincidence probabilities derived by

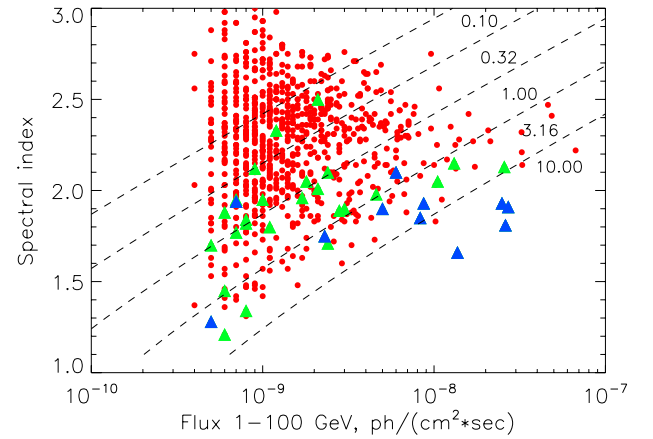


Fig. 3. Comparison of the distribution of fluxes and photon indices of *Fermi* sources of $E \geq 100$ GeV γ -rays (triangles) with those of all sources from the *Fermi* AGN catalog. Blue triangles mark known TeV γ -ray sources.

comparing the expected number of background photons within $\theta \leq 0.12^\circ$ circles (corresponding to the 68% containment circle at 30 GeV) around the sources with the number of source photons in the 30–100 GeV band. For the sources which are detected with more than 5σ significance in the 30–100 GeV band we show more detailed spectra above 1 GeV, calculated using all publicly available data of *Fermi* collected from August 2008 to June 2010 (rather than the 11 month data used for the analysis of the first year *Fermi* catalog). One can see that for most of the sources the estimates of the source flux in the 100–300 GeV energy bin agree well with the extrapolation of the power-law spectrum from lower energies.

The maximum of the correlation signal (minimum of the chance probability) shown in Fig. 2 is achieved at the angle $\theta = 0.17^\circ$, corresponding to the maximum correlation signal in the back-converted events. The improvement in the correlation achieved with the increase of θ from 0.1° to 0.17° means that there are more real events within the rings $0.1 \leq \theta \leq 0.17^\circ$ around their sources, than there are background events in these rings.

Table 2 lists the sources contributing to the correlation signal within $\theta \leq 0.17^\circ$ but not within $\theta \leq 0.1^\circ$. The number of background events in the ring $0.1^\circ \leq \theta \leq 0.17^\circ$ is estimated to be 6. This implies that 6 out of the 25 additional sources listed in Table 2 might be false detections.

We note that only 16 out of 75 sources listed in Tables 1 and 2 are already known sources of VHE γ -rays detected by the ground-based γ -ray telescopes. The majority of the sources from Tables 1 and 2 are new real sources in the VHE band. Taking into account that only 9 out of the 75 sources listed in Tables 1 and 2 are possible false detections, the *Fermi* all sky survey at the energy $E_\gamma \geq 100$ GeV reveals $75 - 9 - 16 = 50$ new extragalactic VHE γ -ray sources. This doubles the number of already known extragalactic VHE γ -ray sources⁴.

Another important point is that the $E \geq 100$ GeV γ -ray sources listed in Tables 1 and 2 are distributed over a broad range of redshifts. The “record” redshift of the VHE γ -ray source so far was $z \approx 0.5$ for the possible detection of 3C 279 during a short several hour flare by MAGIC (Albert et al. 2008). In our Table 1, several sources have redshifts higher than 0.5.

⁴ See <http://tevcat.uchicago.edu/>

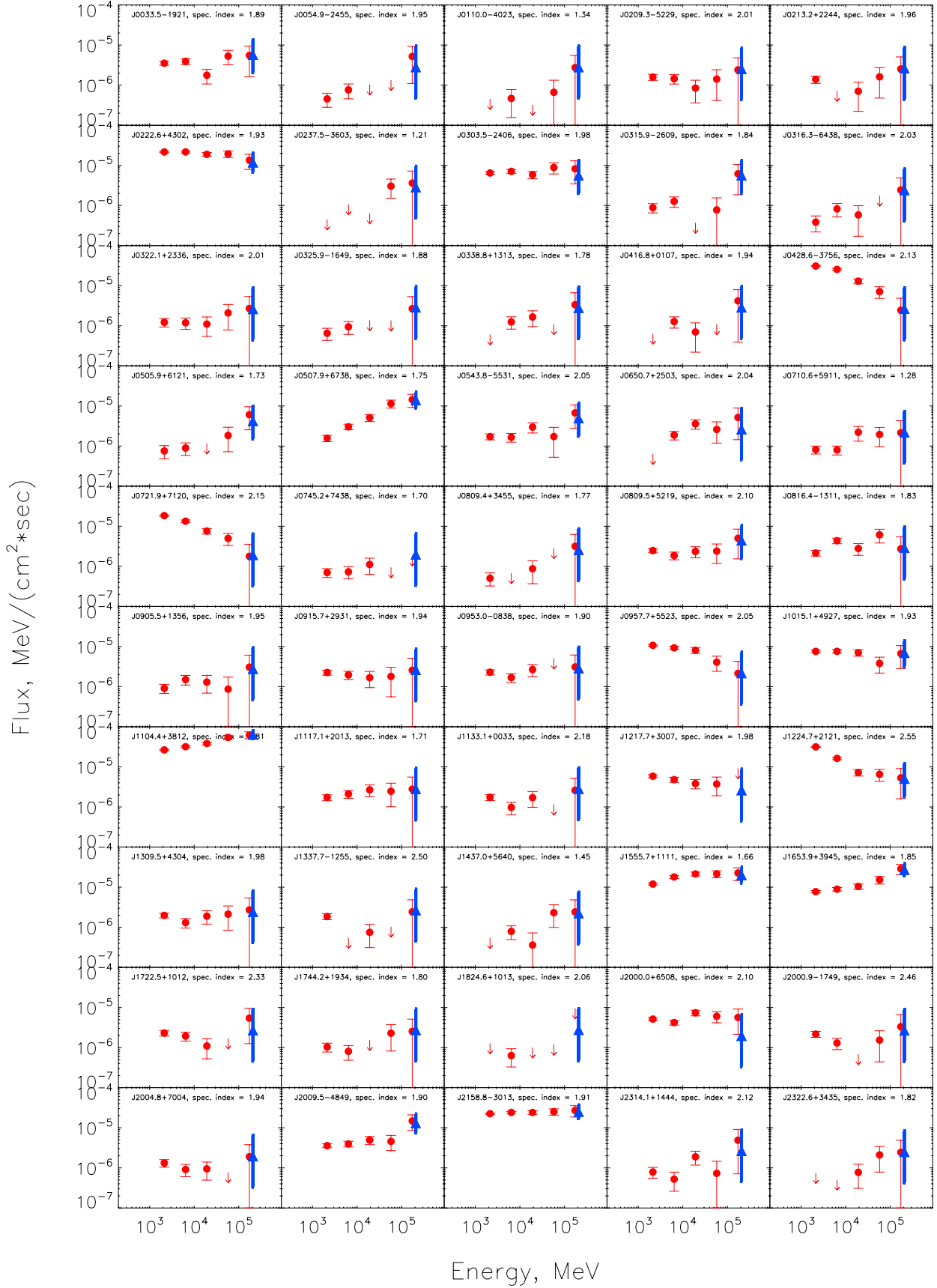


Fig. 4. Comparison of the spectra of the sources from Table 1 in the 1–300 GeV band, obtained with a standard Fermi analysis procedure (red circles represent the flux measurements, red arrows – upper limits), and the estimated source fluxes in the 100–300 GeV band, obtained using aperture photometry technique (blue triangles). Aperture photometry data points in the 100–300 GeV band are artificially shifted to slightly higher energy to ensure that they are visible, and displayed with the measurements from the likelihood analysis in the same energy band.

Table 2. List of *Fermi* sources for which a 100 GeV $< E < 300$ GeV photon is found within the radius $\theta = 0.17^\circ$, but not within $\theta = 0.1^\circ$.

	IFGL	RA	Dec	N_{68}	P_{68}	N_{\min}	P_{\min}	Type	Name2	z
				30–100	30–100	100–300	100–300			
51	J0043.6+3424	10.9240	34.4060	1	2×10^{-2}	1f	7.7×10^{-3}			
52	J0203.5+7234	30.8940	72.5747	0	–	1f	7.2×10^{-3}	BL	CGRaBS J0203+7232	
53	J0440.6+2748	70.1738	27.8151	0	–	1f	5.2×10^{-3}		B2 0437+27B	
54	J0442.7-0019	70.6896	-0.3192	0	–	1f	7.5×10^{-3}		PKS 0440-00	
55	J0449.5-4350	72.3783	-43.8383	12	6.5×10^{-30}	1f	7.8×10^{-3}		PKS 0447-439	
56	J0536.2-3348	84.0605	-33.8027	2	1.6×10^{-4}	1f	8.1×10^{-3}	BL Vf	FRBA J0536-3343	
57	J0803.1-0339	120.7800	-3.6544	1	1.1×10^{-2}	1f	3.1×10^{-3}			
58	J0856.6+2103	134.1578	21.0619	1	1.4×10^{-2}	1b	7.8×10^{-3}	FSRQ	OJ 290	2.106
59	J0909.2+2310	137.3005	23.1761	1	1.7×10^{-2}	1b	8.3×10^{-3}	BL V	RX J0909.0+2311	
60	J1101.3+1009	165.3275	10.1569	1	1.6×10^{-2}	1f	7.7×10^{-3}			
61	J1112.8+3444	168.2035	34.7363	0	–	1b	1.2×10^{-2}	FSRQ	CRATES J1112+3446	1.9556
62	J1125.5-3559	171.3949	-35.9978	0	–	2b	2.5×10^{-5}	AGN	CRATES J1125-3557	
63	J1136.9+2551	174.2362	25.8602	2	1.5×10^{-4}	1f	1.1×10^{-2}	BL V	BZB J1136+2550	0.2
64	J1154.0-0008	178.5117	-0.1469	0	–	1b	7.8×10^{-3}			
65	J1253.0+5301	193.2646	53.0245	1	1.9×10^{-2}	1b	8.6×10^{-3}	BL V	CRATES J1253+5301	
66	J1328.2-4729	202.0501	-47.4991	3	1.8×10^{-6}	1f	5.6×10^{-3}			
67	J1345.4+4453	206.3740	44.8965	0	–	1b	7.7×10^{-3}	FSRQ	B3 1343+451	
68	J1426.9+2347	216.7495	23.7987	16	7.5×10^{-43}	2b	2.6×10^{-5}	BL V	PKS 1424+240	0.16
69	J1428.7+4239	217.1790	42.6568	6	1.3×10^{-14}	1b	7.8×10^{-3}	BL V	1ES 1426+428	0.129
70	J1553.9+4952	238.4886	49.8724	2	1.3×10^{-4}	1b	9.8×10^{-3}			
71	J1923.5-2104	290.8849	-21.0771	0	–	1f	9.4×10^{-3}	FSRQ	OV -235	0.874
72	J2014.5-0047	303.6400	-0.7858	1	2×10^{-2}	1b	7.9×10^{-3}			
73	J2250.1+3825	342.5275	38.4328	3	1.6×10^{-6}	1b	7.3×10^{-3}	BL V	3 2247+381	0.1187
74	J2323.5+4211	350.8912	42.1947	5	2.1×10^{-11}	1b	$7. \times 10^{-3}$	BL V	1ES 2321+419	
75	J2325.8-4043	351.4613	-40.7184	1	1.4×10^{-2}	1b	$8. \times 10^{-3}$	BL V	RXS J23247-4040	

Notes. Notations are the same as in Table 1.

5. Correlation between arrival directions of 100 GeV $\leq E \leq 300$ GeV photons and sources from the 13th Veron catalog

Most of the 100 GeV $\leq E \leq 300$ GeV sources listed in Tables 1 and 2 are BL Lac objects. These sources are known to be characterized by relatively hard spectra in the GeV energy band (Abdo et al. 2010c). It is therefore possible that some of the VHE γ -ray emitting BL Lacs escape detection in the GeV band, while being bright VHE γ -ray sources.

To search for the VHE γ -ray emitting BL Lacs with very hard spectra, we performed a correlation analysis similar to the one reported above for the first year *Fermi* catalog also for the 13th Veron catalog of BL Lacs (Veron-Cetty & Veron 2010). To select a complete sample of BL Lacs, we adopted the prescription of Gorbunov et al. (2005) and applied a cut to magnitude of objects $V < 18.0$, which leaves 316 BL Lacs. This set of objects includes six out of seven known VHE γ -ray sources identified in the $E \geq 100$ GeV *Fermi* data by Neronov et al. (2010). As in the analysis of the first year *Fermi* catalog, we removed those objects and associated photons from analysis. We also removed the three photons associated with IC 310. This leaves $N_{\text{source}} = 310$ BL Lac objects and 3111 photons.

The probability that a single photon comes by chance near one of the selected BL Lacs is $p = N_{\text{source}} \cdot p_1 = 2.7 \times 10^{-4} \cdot (\theta/0.1^\circ)^2$. The probability that K or more photons fall within an angle θ from one of the sources is calculated using Eq. (3). Figure 5 shows this chance probability as a function of θ . As for the analysis of first year *Fermi* source catalog, the probability has a minimum at the angular resolution of the LAT at the energies $E \geq 100$ GeV. From our correlation analysis we find that 39 BL Lac out of 310 correlate with *Fermi* data within the angle

$\theta \lesssim 0.17^\circ$ corresponding to the minima of $P(\theta)$ from Figs. 1 and 5.

In Fig. 6, we compare the number of source photons to the number of background photons as functions of the angular distance to the BL Lacs. The asymptotic value of the signal events $N = 54$ is reached at the angular distance $\sim 0.2^\circ$. At the angle 0.1° , 31 photons come from 28 sources, while only 0.9 of them are on average caused by the background. At 95 % C.L., there are two background photons. At the angular distance 0.17° , 47 photons come from 39 sources, and 2.6 of them correspond to background in average. There are 5[6] background photons at the 95%[99%] confidence level. Eight of these 35 sources are not present in Tables 1 and 2. These seven sources are listed in Table 3. Other sources contributing to the correlation signal in both the first year *Fermi* and Veron-Cetty & Veron (2010) catalogs are marked by an ‘‘V’’ in Tables 1 and 2.

We also performed a special analysis with only front photons and a BL Lac catalog. In this case, the correlation signal is maximal at $\theta \simeq 0.07^\circ$ (see Fig. 5). At this angle, there are 21 forward photons, which correlate with 20 BL Lac sources. PKS 0301-243 has two photons, which can occur by chance in only $P = 10^{-7}$ cases. This means that this source is discovered by *Fermi*. Only 0.18 background photons are expected at this angle, which means that all of the 19 remaining sources are most probably real. At the 99% confidence level, two of the 20 sources might be false detections. Sixteen of these 20 sources are marked as ‘‘Vf’’ in Tables 1 (15 sources) and 2 (1 source) and the remaining six are those have front photons marked ‘‘f’’ in Table 3.

6. Sources at energies $E > 300$ GeV

We discuss correlations between 900 *Fermi* photons with $E > 300$ GeV and sources from the first year *Fermi* catalog and

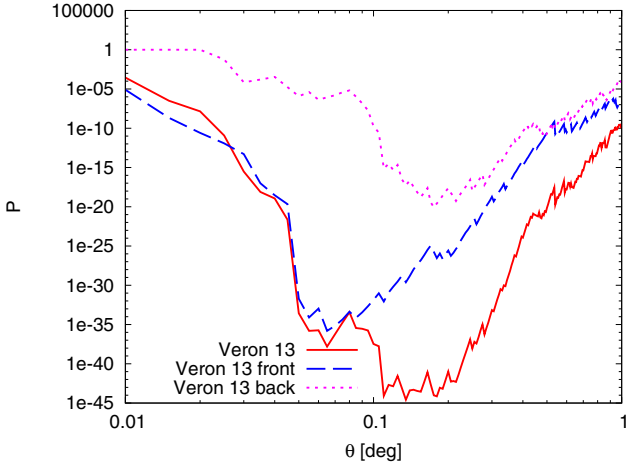


Fig. 5. Dependence on the chance probability of correlation between arrival directions of $100 \text{ GeV} \leq E \leq 300 \text{ GeV}$ photons and positions of BL Lacs from Veron-Cetty & Veron (2010) catalog as a function of the radius of the search circle. Notations are the same as in Fig. 1.

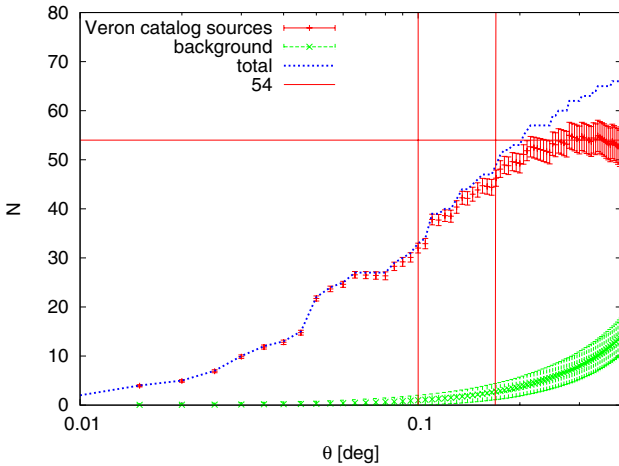


Fig. 6. Number of events which come from BL Lac sources as a function of the radius of the search circle. Notations are the same as in Fig. 2.

BL Lacs from Veron-Cetty & Veron (2010) catalog. We note that this energy is exactly in the range of sensitivity of the TeV gamma-ray telescopes.

We first consider correlations with sources from the first year *Fermi* catalog. Using an analysis identical to the one presented in Sect. 3, we study correlations of $E > 300 \text{ GeV}$ photons with the sources within a $\theta = 0.1^\circ$ angular distance. There are four sources correlated within this angle, while only 0.7 photons are expected to be found in the direction of *Fermi* sources in the case of random coincidences. Those sources are presented in the first four lines of Table 4. All of them are known TeV sources.

We next consider correlations of photons with $E > 300 \text{ GeV}$ with sources from the first year *Fermi* catalog within $\theta = 0.17^\circ$ in analogy with Table 2. There is one more source (source # 5 in Table 4) that correlates with $E > 300 \text{ GeV}$ photons within this angle but does not correlate within $\theta = 0.1^\circ$. We expect 2.3 background events within this angle. The $E > 300 \text{ GeV}$ photons from the direction toward source # 5 is, most probably, a random coincidence, because this source is a blazar at the redshift $z > 1$. Photons with $E > 300 \text{ GeV}$ cannot reach the Earth from a source at such high redshift because of the interactions with the infrared background.

Table 3. List of BL Lac sources from Veron-Cetty & Veron (2010) catalog for which a $100 \text{ GeV} \leq E \leq 300 \text{ GeV}$ photon is found within the circle of radius 0.1° and are not the first year *Fermi* catalog sources.

	Name	RA deg	Dec deg	$N_{0.1}$ [N_{\min}]	z
1	<u>NPM1G +01.0067</u>	28.165	1.788	1f	0.08
2	V Zw 326	48.210	36.256	1b	0.071
3	B3 0651+428	103.682	42.799	1f	0.126
4	<u>RXS J09130-2103</u>	138.252	-21.054	1f[1b]	0.198
5	RXS J10162+4108	154.070	41.137	1b	0.281
6	SDSS J114023.48 +152809.7	175.098	15.469	1f	0.244
7	MS 12218+2452	186.101	24.607	1f	0.218
8	MS 13121-4221	198.764	-42.614	1f	0.105

Notes. Underlined source is detected by *Fermi* in $100\text{--}300 \text{ GeV}$ band with $TS > 25$. Column 5 gives the number of photons in the circles of the radius 0.1° and 0.17° around the source ($N_{0.1}$ and N_{\min} , respectively). Column 6 is the source redshift.

Table 4. List of *Fermi* and BL Lac sources from Veron-Cetty & Veron (2010) catalog for which a $E > 300 \text{ GeV}$ photon is found within the circle of radius 0.17° .

	Name	RA	Dec	$N_{0.1}$	N_{\min}	z
1	<u>1ES 0502+675</u>	76.99	67.64	1f 1b	1b	0.341
2	<u>Mkn 421</u>	166.1	38.21	1f 3b	1f	0.03
3	<u>B2 1218+30</u>	185.3	30.18	1f	1f	0.184
4	<u>1ES 1959+650</u>	300.0	65.13	1b		0.048
5	RGB J0250+172	42.66	17.20		1b	1.1
6	SHBL J10102-3119	152.6	-31.32	1b		0.143

Notes. Underlined sources are detected with *Fermi* at $E > 300 \text{ GeV}$ energies with $TS > 25$. Notations are the same as in Table 3.

We can finally repeat the analysis of Sect. 5 and consider correlations with BL Lacs from Veron-Cetty & Veron (2010) catalog. We find that there are photons correlating with four out of 317 bright BL Lac sources with magnitude $V < 18$ within $\theta = 0.1^\circ$. Those are sources 2, 3, 4, and 6 in Table 4. In this case, only 0.27 background photons are on average expected. The only new source is source number 6, which is more probably a real source rather than a random coincidence (with probabilities 0.73 vs. 0.27 for the two cases). At the same time, the source is located at a moderate Galactic latitude, 20° , so that the possibility that an excess at the position of the source is due to the diffuse emission from the Galaxy cannot be ruled out.

7. Comments on individual sources

7.1. High redshift sources

Several sources in Table 1 have redshifts higher than the redshift of 3C 279, $z \approx 0.5$, which is the furthest known VHE γ -ray source (Albert et al. 2008). The study of high redshift sources in the VHE band is interesting for the measurements of the density and cosmological evolution of the extragalactic background light (EBL) (Gould & Schreder 1967; Kneiske et al. 2004; Stecker et al. 2006; Mazin & Rau 2007; Franceschini et al. 2008) and the cosmological magnetic fields (Neronov & Semikoz 2009; Neronov & Vovk 2010). In this subsection, we provide some details about the high redshift sources from Table 1.

RBS 76 at $z = 0.61$ has two photons within the distance 0.17° from the catalog source position. It is detected with a

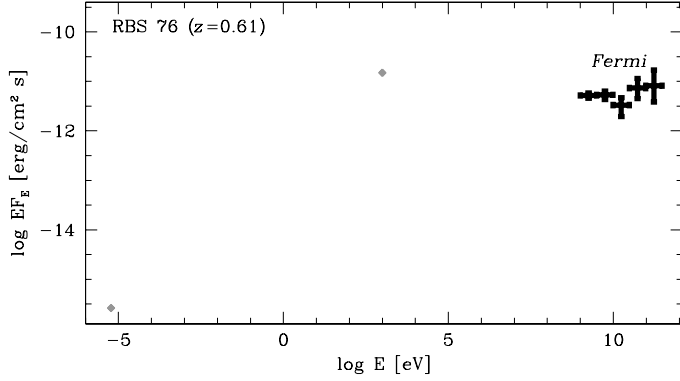


Fig. 7. Broad-band spectrum of RBS 76. Grey data points are historical data from NED.

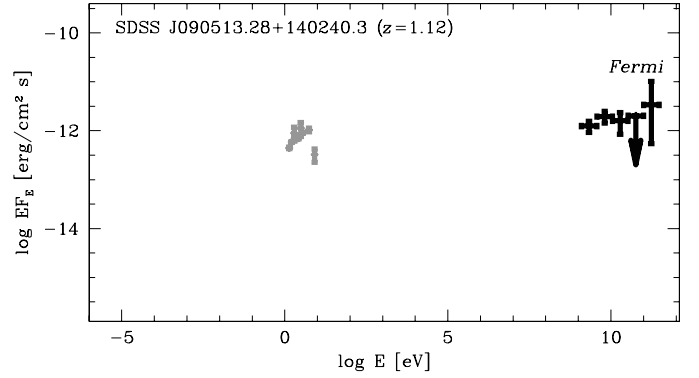


Fig. 9. Broad-band spectrum of SDSS J090513.28+140240.3. Grey data points show historical data from NED.

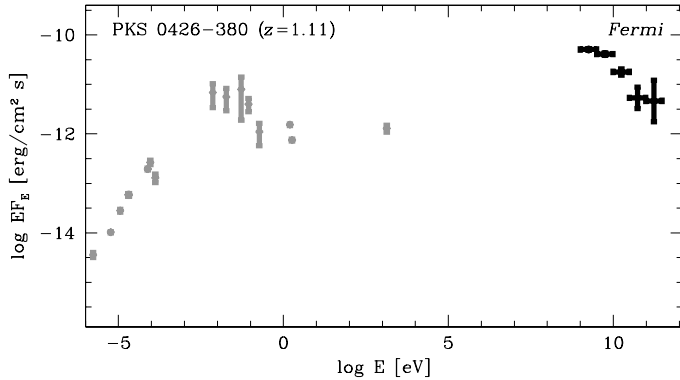


Fig. 8. Broad band spectrum of PKS 0426-380. Grey data points show historical data taken from NED.

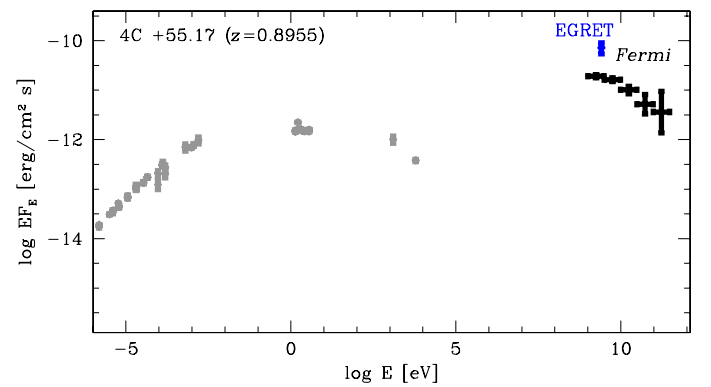


Fig. 10. Broad-band spectrum of 4C +55.17. Grey data points show historical data from NED. Blue data point is the measurement of γ -ray flux by EGRET (Thompson et al. 1995).

of significance more than 4σ in the 100–300 GeV band. The source is also detected with a significance of more than 7σ in the 30–100 GeV energy band.

Broad band spectrum of the source is shown in Fig. 7. The historical multiwavelength data are taken from the NASA Extragalactic Database (NED)⁵.

PKS 0426-380 at $z = 1.11$ is a bright source in the GeV energy band, with the flux reaching 10^{-10} erg/cm² s. Its γ -ray spectrum is relatively soft and consistent with a power-law with photon index $\Gamma \geq 2.5$. The γ -ray measurements are compared to the multiwavelength data for the source in Fig. 8. As in the case of RBS 76, the overall spectrum of the source could be interpreted in terms of the synchrotron self-Compton or synchrotron external-Compton type models where the radio-to-optical emission is produced by means of the synchrotron mechanism and X-ray-to- γ -ray emission by inverse Compton scattering. The extremely high redshift of the source and possible presence of the high-energy cut-off in the spectrum might increase the difficulty of the source detection with ground-based γ -ray telescopes at energies significantly higher than 100 GeV.

SDSS J090513.28+140240.3 at $z = 1.12$ has a flat (E^{-2}) spectrum in the 1–300 GeV band. It was previously only observed in the optical domain. A comparison of γ -ray measurements and historical data is presented in Fig. 9. The extrapolation of the source spectrum from energies below 100 GeV agrees well with the estimated flux in the 100–300 GeV band, giving no indication of a cutoff. Despite the low statistics in the data for this band

obtained with *Fermi*/LAT, this means that the source should be observable with ground-based Cherenkov telescopes.

4C +55.17 at $z = 0.8955$ also has a relatively soft spectrum in the 1–300 GeV band. The γ -ray measurements are compared to the broad-band data in Fig. 10. The source was previously detected in the 0.1–1 GeV band by EGRET. There are no other sources from the first year *Fermi* catalog within a distance 4° of the source. This means that an EGRET measurement most probably refers to the same blazar, rather than to a possible nearby higher flux source. A comparison of the historical EGRET measurement with the *Fermi* measurement of the source flux shows that the source is variable on a 10 yr timescale.

PKS B1130+008 at $z = 1.223$ has the second highest redshift among the sources listed in Table 1. It has an associated front-converted photon with energy 128 GeV. An estimate of the source flux above 100 GeV based on this one photon is above the extrapolation of the source spectrum from the lower energies; we refer to Fig. 11 which possibly indicates that this high redshift source is a false detection. Otherwise, if the source spectrum is flat at energies up to 100 GeV, as indicated by the detection of the $E > 100$ GeV γ -ray, its observation with the ground-based Cherenkov telescopes should provide valuable constraints on the EBL at redshifts $z \sim 1$.

B3 1307+433 at $z = 0.69$ has a harder than E^{-2} spectrum up to the highest energies accessible to *Fermi* (see Fig. 12). The estimate of the flux based on the detected $E > 100$ GeV photon agrees well with the extrapolation of the source spectrum from

⁵ <http://nedwww.ipac.caltech.edu/>

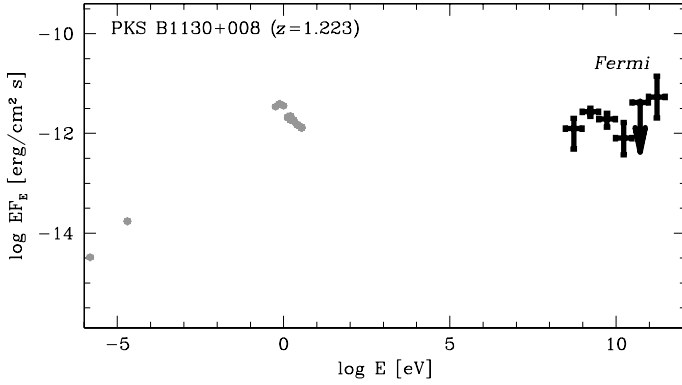


Fig. 11. Broad-band spectrum of PKS B1130+008. Grey data points show historical data from NED.

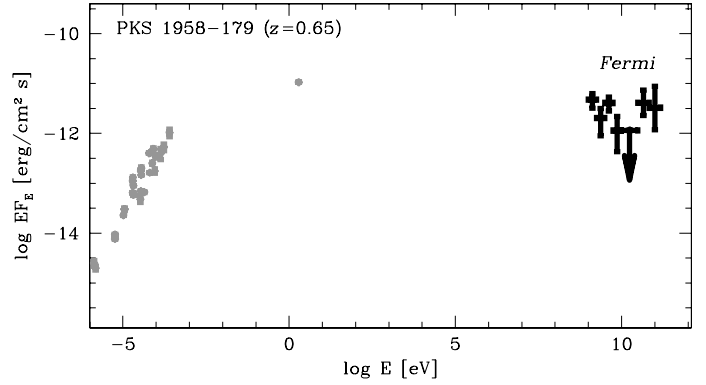


Fig. 13. Broad-band spectrum of PKS1958-179. Grey data points show historical data from NED.

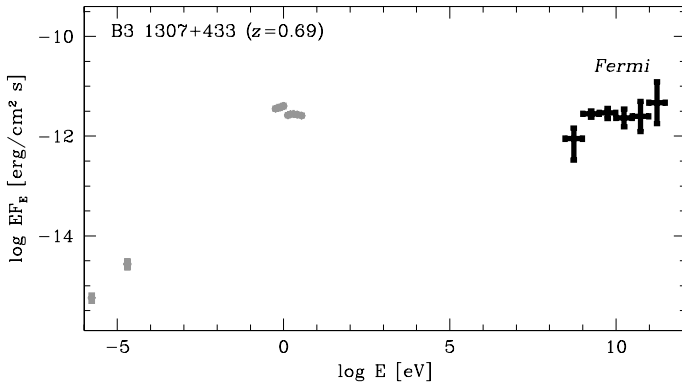


Fig. 12. Broad-band spectrum of B3 1307+433. Grey data points indicate historical data from NED.

lower energies. This indicates that the source should be readily detectable with ground-based γ -ray telescopes, despite its high redshift.

PKS 1958-179 at $z = 0.65$ is also characterized by an excess of high-energy ($E > 30$ GeV) emission above the extrapolation of the lower energy spectrum with $\Gamma = 2.46 \pm 0.07$ reported in the first year Fermi catalog. No photons are indeed detected from the source in the energy range 10–30 GeV (see Fig. 13). However, at the energies above 30 GeV the source is clearly identifiable in Fermi count maps (see Fig. 14). Standard likelihood analysis gives TS value $TS = 32$, which formally corresponds to $>5\sigma$ detection in this energy range. This indicates that the source spectrum hardens at the energies above 30 GeV. Unfortunately, the statistic of the Fermi signal at the highest energies is insufficient to clarify the nature of the 100 GeV excess in the source spectrum.

BZU J2313+1444 is formally the highest redshift source in Table 1, with $z = 1.319$. The source is relatively weak. In contrast to the other high-redshift sources, the significance of source detection in the 30–100 GeV band is less than 5σ . From Fig. 15, one can see that the source spectrum does not exhibit a signature of a high energy cut-off. This implies that the source might be an ideal candidate for the study of EBL evolution with redshift.

7.2. Sources detected at $\geq 4\sigma$ level at $E \geq 100$ GeV

Apart from the eight high-confidence sources at $E \geq 100$ GeV found by Neronov et al. (2010) and the bright high-redshift

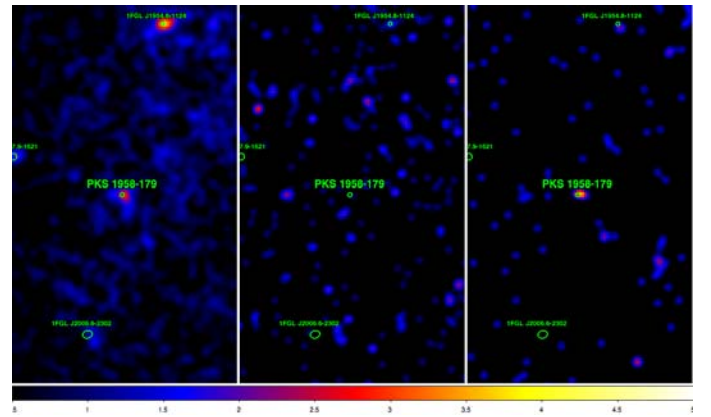


Fig. 14. LAT count maps smoothed by 0.3° around the position of PKS 1958-179 in 1–10 GeV (left), 10–30 GeV (center), and 30–300 GeV (right) bands. Color scales are linear, from 0.5 to 5 counts per pixel (left panel), from 0.04 to 0.4 cts/pixel (center), and from 0.03 to 0.3 cts/pixel (right panel).

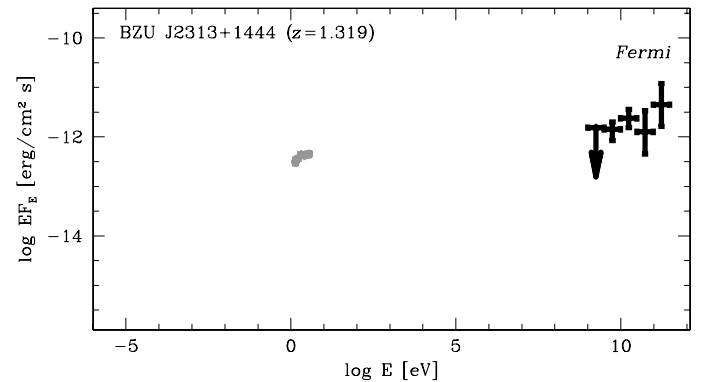


Fig. 15. Broad-band spectrum of BZU J2313+1444. Grey data points show data from NED.

sources discussed above, several other sources in Tables 1 and 2 have detection significances higher than 4σ above 100 GeV. We list below these sources and discuss some details of their broad-band spectral energy distribution.

PKS 0301-243 at $z = 0.26$ has one back- and two front-converted photon associated with the source above 100 GeV. The back photon is within the 95% containment circle of the radius $\theta = 0.3^\circ$. Taken together, the two photons represent a $\approx 5.2\sigma$ detection of the source above 100 GeV. At the same

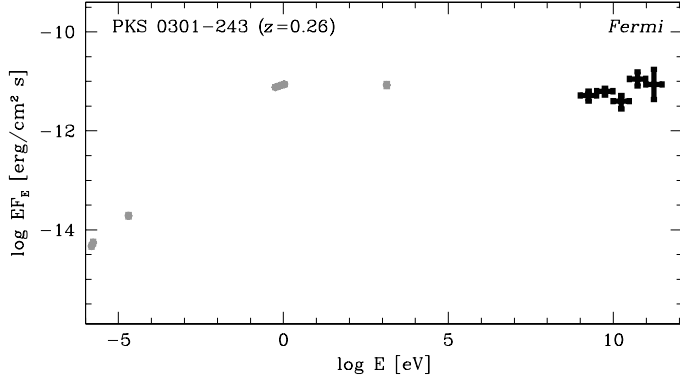


Fig. 16. Broad-band spectrum of PKS 0301-243. Grey color shows historical data from NED.

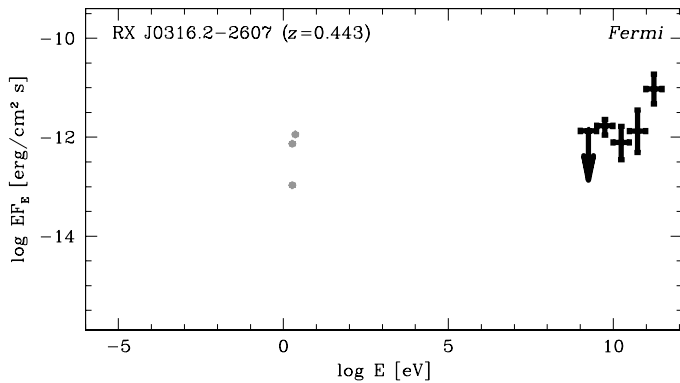


Fig. 17. Broad-band spectrum of RX J0316.2-2607. Grey color shows historical data from NED.

time, the source is also detected with high significance in the 30–100 GeV band. Both $E > 100$ GeV photons came during the flaring activity of the source in April–May 2010 (Cannon 2010; Neronov et al. 2010d). The broad-band spectrum of PKS 0301-243, shown in Fig. 16, is consistent with the possibility that radio-to-X-ray emission are produced via the synchrotron mechanism and the 1–300 GeV emission via the inverse Compton mechanism.

RX J0316.2-2607 is a relatively high redshift ($z = 0.443$) source, which has two back γ -rays within the distance $\theta = 0.1^\circ$. The chance coincidence probability of finding two photons within this distance from the source is 2.5×10^{-6} , which implies a detection significance 4.7σ above 100 GeV. From Fig. 17, one can see that the source has a hard γ -ray spectrum without a signature of a high-energy cut-off. The γ -ray energy flux from the source is comparable to the optical flux. Similarly to BZU J2313+1444, this source might also be an ideal candidate for the study of both EBL and cosmological magnetic fields.

1FGL J0505.9+6121 has three adjacent photons within 0.22° . Formally, the chance probability of finding three photons inside this distance is $P = 8 \times 10^{-8}$; however, since the detection angle was not defined a priori, it has to be penalized for this and the final probability is just 5σ (see Table 1), still implying that the source is detected at $E \geq 100$ GeV individually, and not only within the population of *Fermi* sources from Table 1. It is also detected with a significance higher than 5σ in the 30–100 GeV band. The spectrum of the source shown in Fig. 18 is consistent with a hard power-law (photon index harder than 2) up to the highest energy.

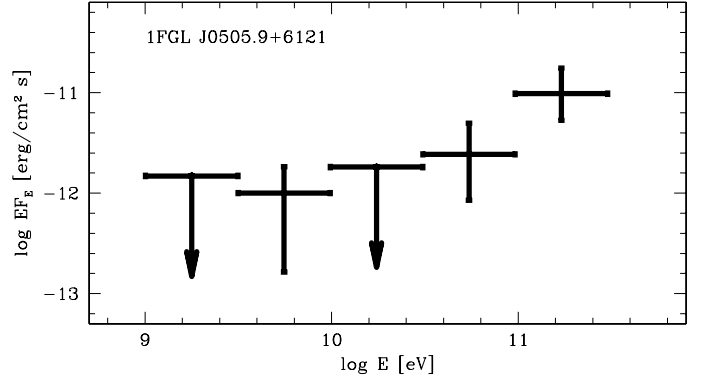


Fig. 18. *Fermi* spectrum of 1FGL J0505.9+6121.

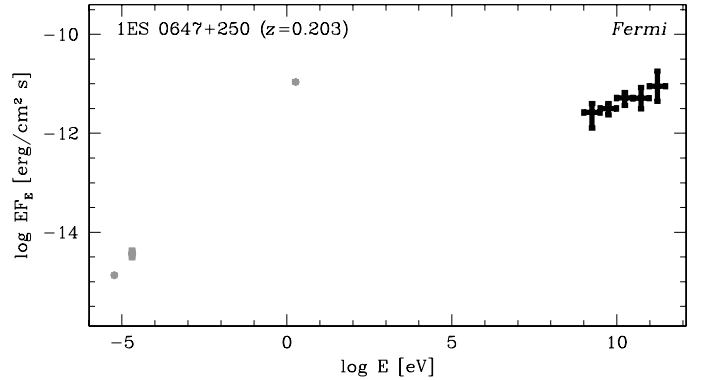


Fig. 19. Broad-band spectrum of 1ES 0647+250. Grey color shows historical data from NED.

The object is located near the Galactic plane at $b = +12^\circ$, so that it can be of Galactic origin. The high level of Galactic diffuse γ -ray background around the location of the source prevents its detection at lower energies $E \leq 1$ GeV. The small value of the test-statistics (TS) value⁶ for this source in the Table 1 could indicate that this source is not point-like. A standard *Fermi*/*LAT* analysis procedure, which was used to calculate the value of TS, does not work in this case.

Detailed multiwavelength observations are needed to constrain its nature. A possible candidate for the source identification is the radio- and X-ray loud AGN RX J0505.9+6113 (Brinkman et al. 1997) situated at the distance $7.6'$ from the catalog source position and the distance 0.06° from the front-converted $E \geq 100$ GeV photon.

1ES 0647+250 at $z = 0.201$ was already mentioned as a “candidate” TeV blazar in the analysis of Costamante & Ghisellini (2002), based on its broad-band spectra properties. Figure 19 demonstrates that the source has a hard γ -ray spectrum, with no signature of a cut-off up to 300 GeV. This ensures that it should be readily detectable with ground-based γ -ray telescopes.

4C +21.35 at $z = 0.432$ is an intermediate redshift BL Lac that exhibited a γ -ray flare in April–May 2010 (Donato 2010) during which both $E > 100$ GeV photons associated with the source were detected, resulting in the detection of the source with 5.6σ significance above 100 GeV (Neronov et al. 2010a). The detection of the source above 100 GeV was recently confirmed with MAGIC observations of the source (Mariotti 2010). A time-averaged spectrum of the source in the 1–300 GeV band

⁶ See <http://fermi.gsfc.nasa.gov/ssc/data/analysis/scitools>

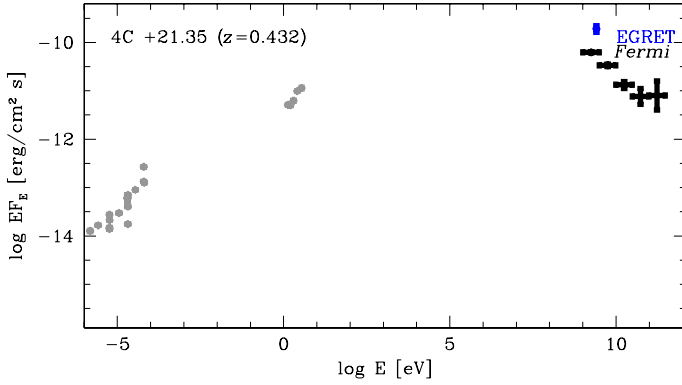


Fig. 20. Broad-band spectrum of 4C +21.35. Grey color shows historical data from NED. Blue point is EGRET measurement.

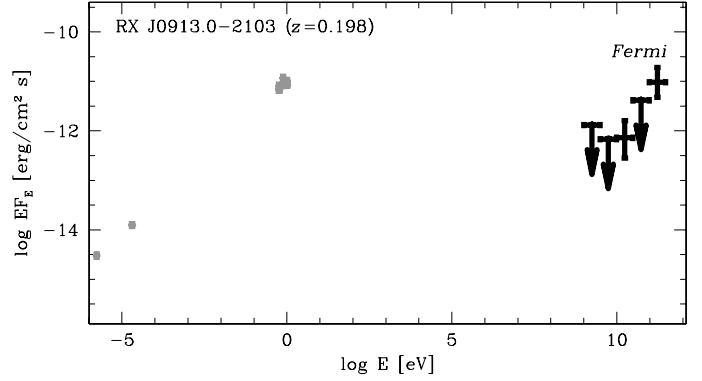


Fig. 22. Broad-band spectrum of RX J0913.0-2103. Grey data points show historical data from NED.

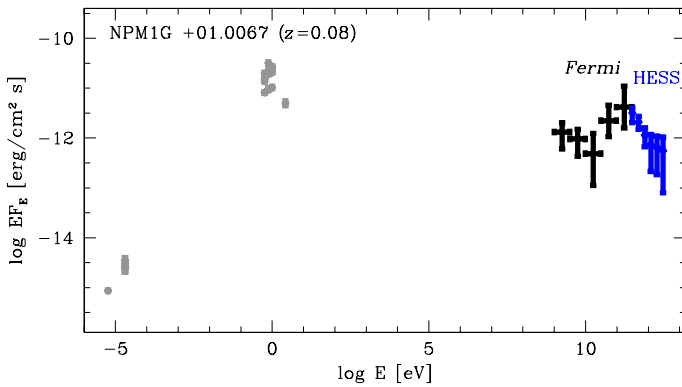


Fig. 21. Broad-band spectrum of NPM1G +01.0067. Grey color shows historical data from NED.

is shown, together with the historical data, in Fig. 20. The previous EGRET measurement of the source flux is characterized by a somewhat higher source flux. This indicates that the source is variable not only on the short (days to month) timescale, but also on decade-long timescales.

7.3. Sources from the BL Lac catalog

NPM1G+01.0067 at $z = 0.08$ was previously detected in the VHE band by HESS (Aharonian et al. 2008). The *Fermi* spectrum of the source, shown in Fig. 21 is in good agreement with the HESS measurements. In spite of the source not being reported in the first year *Fermi* catalog, it is detected in the 1.9 yr exposure with a TS value of $TS = 108$ above 1 GeV.

RX J09130-2103 has two γ -rays with energies $E \geq 100$ GeV within 0.1° distance. One of the γ -rays is a front-converted γ -ray, for which the 68% containment circle has a smaller radius. The front-converted γ -ray is at the distance 0.01° from the catalog source position and a back photon at 0.03° . The field of the radius 10° around the source contains 20 photons at the energies above 100 GeV. The overall chance probability of finding front- and back-converted photons within the 68% containment circles of the front-converted and back-converted photons is $\approx 10^{-5}$.

Despite the source not being reported in the first year *Fermi* catalog, it is also detected with *Fermi* at energies below 100 GeV. A standard likelihood analysis in the energy range 1–300 GeV gives the TS value 80, which corresponds to a source detection significance $\approx 9\sigma$.

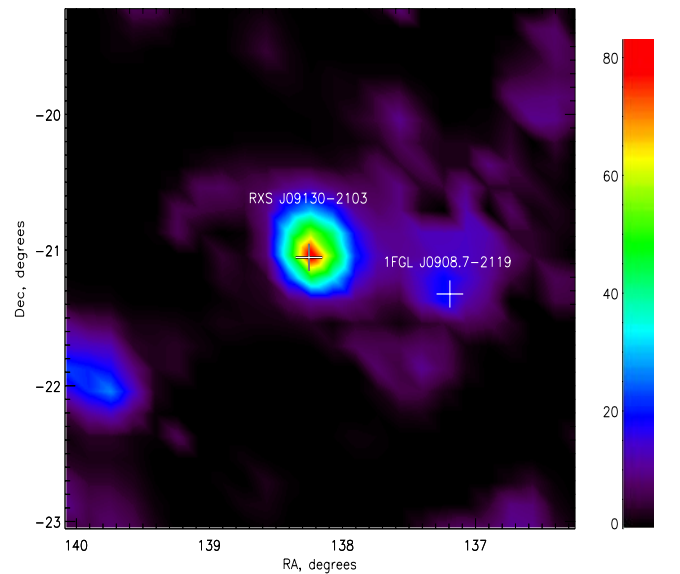


Fig. 23. TS map of the region $2^\circ \times 2^\circ$ in the energy band above 1 GeV around the position of RX J0913.0-2103.

The map of TS values in the region $2^\circ \times 2^\circ$ around the source is shown in Fig. 23. The TS values were calculated for the model of source distribution in the region 14° around RX J09130-2103 in which all the first year *Fermi* source catalog sources apart from 1FGL J0908.7-2119 were included and one additional source was allowed to have a variable position. One can see that the TS value at the position of RX J09130-2103 is much larger than that at the position of 1FGL J0908.7-2119, which is only marginally detected above 1 GeV.

The broad-band spectrum of the source is shown in Fig. 22. One can see that the γ -ray spectrum of the source is hard, which explains its non-detection in the first 11 months of operation of *Fermi*.

MS 12218+2452 has a front-converted photon at the distance 0.04 from the catalog source position. The source is also not reported in the first year *Fermi* catalog, but is detected in the 1.5 yr exposure with TS value 80, which corresponds to the $\approx 9\sigma$ significance of the source detection.

The map of TS values in the region of size $1^\circ \times 1^\circ$ at energies $E \geq 1$ GeV around the source position is shown in Fig. 25. To construct this map, we included all the sources from the first year *Fermi* catalog situated at the distance $\theta \leq 14^\circ$ from the source

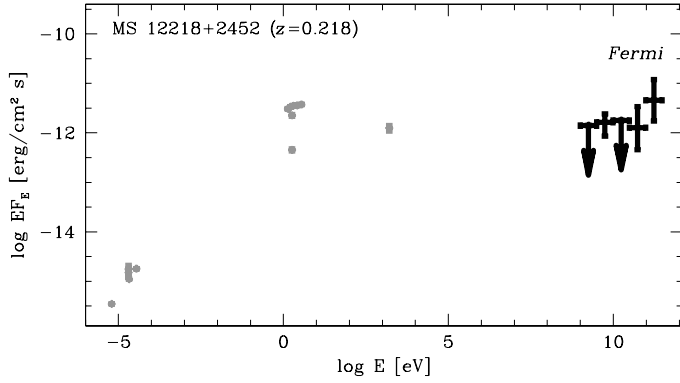


Fig. 24. Broad-band spectrum of MS 12218+2452. Grey data points show historical data from NED.

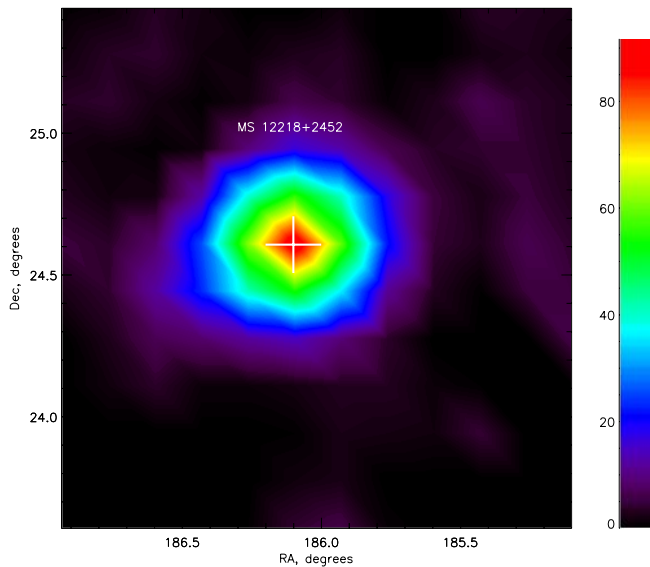


Fig. 25. TS map of the region $1^\circ \times 1^\circ$ in the energy band above 1 GeV around the position of MS 12218+2452.

position into the model of source distribution on the sky. One can clearly see the source in the TS map.

Fermi data are compared to the broad-band archival data in Fig. 24. The γ -ray flux from the source is comparable to its optical flux intensity. The γ -ray spectrum does not display any signatures of a high-energy cut-off.

8. Discussion and conclusions

The study of cross-correlation of the arrival directions of the highest energy photons ($E \geq 100$ GeV) detected by *Fermi* with the catalog of sources detected at lower energies $E < 100$ GeV has proven to be an efficient way of finding new γ -ray sources observable in the VHE γ -ray band. This study complements the pointed observations of selected γ -ray sources with the ground-based γ -ray telescopes because it results in an all-sky survey of the high Galactic latitude VHE γ -ray sky.

The high Galactic latitude sky survey above 100 GeV has revealed a large number of new VHE γ -ray sources. Adding the list of new sources to that of all sources previously detected with the ground-based γ -ray telescopes doubles the number of known extragalactic VHE γ -ray sources. As for all known VHE γ -ray sources, most of the new sources reported

in Tables 1–3 are BL Lac type objects, a special type of AGN with jets closely aligned to the line of sight.

The majority of the sources listed in Table 1 are real new VHE γ -ray sources; only three sources are expected to be false detections caused by the chance coincidence of arrival directions of γ -rays with the source position. Several sources in Table 1 have more than one photon associated with them. These sources are detected with high significance in the energy range 100–300 GeV. Sources correlating with only one $E > 100$ GeV photon should be considered as “VHE source candidates”. Apart from the known VHE γ -ray sources, the unidentified *Fermi* source 1FGL J0505.9+6121 as well as PKS 0301-243 and 4C +21.35 is detected with a significance close to 5σ above 100 GeV. In addition, BL Lacs with an associated front-converted photon, which are found to correlate with the Veron-Cetty & Veron (2010) catalog (marked by “Vf” in Table 1), should also be considered as high-confidence detections.

Table 2 lists 21 lower significance sources, among which five or six are most probably false detections. As for Table 1, the source marked “Vf” (# 56) which contributes with a front-converted photon to the correlation with the BL Lac catalog should be considered as a higher significance detection. For the sources listed in this table, it is reasonable to accumulate longer exposure to single out false detections.

Table 3 lists VHE γ -ray emitting BL Lacs that were not listed in the first year *Fermi* catalog, but contribute to the correlation of the *Fermi* VHE γ -rays with the BL Lac catalog of Veron-Cetty & Veron (2010). Their absence from the *Fermi* catalog might be caused by the hard spectra of these sources. We have demonstrated that three of the eight sources listed in Table 3, the sources # 1, 4, and 7 are, in fact, detected with a significance $>5\sigma$ in the 1–300 GeV band. The other three sources which have a front-converted photon associated with them should also be considered as probable true detections.

Table 4 lists six sources, which have photons with energies above 300 GeV, including four known TeV sources and two possible new sources which are, however, consistent with random coincidences with background photons. Among the TeV sources, only B2 1218+30 does not contain photons in the 100–300 GeV energy range within a region $\theta \leq 0.2^\circ$ about its center. However it has 2 back-converted photons at $0.2^\circ < \theta < 0.3^\circ$.

Some of the new VHE γ -ray sources listed in Table 1 is situated at high redshifts $z \sim 1$. Our analysis of the γ -ray spectra of the high redshift sources indicates that at least several of them do not display any signatures of a high-energy cut-off up to 300 GeV. The typical fluxes of the sources listed in Tables 1–3 are at the level $EF_E(E \geq 100 \text{ GeV}) \geq (\text{few}) \times 10^{-12} \text{ erg}/(\text{cm}^2 \text{ s})$, i.e., at the level of 0.1 Crab units. These sources should be readily detectable by ground-based Cherenkov telescopes at energies of several hundreds of GeV. The larger collection area of the ground-based telescopes should result in much higher quality signal statistics, which should allow a study of the detailed spectral properties of these new bright VHE γ -ray sources. We anticipate that a detailed high sensitivity study of high-redshift VHE γ -ray sources with ground-based γ -ray telescopes will enable us to study the cosmological evolution of the BL Lac properties, the EBL, and the associated evolution of galaxies producing the EBL (Gould & Schreder 1967; Kneiske et al. 2004; Stecker et al. 2006; Mazin & Raue 2007; Franceschini et al. 2008), as well as cosmological intergalactic magnetic fields (Neronov & Semikoz 2009; Neronov & Vovk 2010).

Acknowledgements. We would like to thank Igor Tkachev and Peter Tinyakov, who performed an analysis similar to the one described in Sect. 5 and pointed out to us that we can also use data with $E > 300$ GeV obtained by *Fermi*. The work of A.N. and Ie.V. is supported by the Swiss National Science Foundation grant PP00P2_123426.

References

- Abdo, A. A., Ackermann, M., Ajello, M., et al. 2010a, *ApJS*, 88, 405
 Abdo, A. A., Ackermann, M., Ajello, M., et al. 2010b, *ApJ*, 720, 435
 Abdo, A. A., Ackermann, M., Ajello, M., et al. 2010c, *ApJ*, 715, 429
 Aharonian, F. A., Akhperjanian, A. G., Aye, K.-M., et al. 2005, *Science*, 307, 1938
 Aharonian, F. A., Akhperjanian, A. G., Bazer-Bachi, A. R., et al. 2006, *ApJ*, 636, 777
 Aharonian, F. A., Akhperjanian, A. G., Barres de Almeida, U., et al. 2008, *A&A*, 481, L103
 Albert, J., Aliu, E., Anderhub, H., et al. 2008, *Science*, 320, 1752
 Amenomori, M. 2005, *ApJ*, 633, 1005
 Atkins, R., Benbow, W., Berley, D., et al. 2004, *ApJ*, 608, 680
 Atwood, W. B., Abdo, A. A., Ackermann, M., et al. 2009, *ApJ*, 697, 1071
 Brinkman, W., Siebert, J., Feigelson, E. D., et al. 1997, *A&A*, 323, 739
 Cannon, A. 2010, *ATEL*, 2591
 Costamante, L., & Ghisellini, G. 2002, *A&A*, 384, 56
 Dingus, B. L., & Bretsch, D. L. 2001, *AIP Conf. Proc.*, 587, 251
 Donato, D. 2010, *ATEL*, 2584
 Franceschini, A., Rodighiero, G., & Vaccari, M. 2008, *A&A*, 487, 837
 Gorbunov, D. S., Tinyakov, P. G., Tkachev, I. I., & Troitsky, S. V. 2005, *MNRAS*, 362, L30
 Gould, R. J., & Schreder, G. P. 1967, *Phys. Rev. Lett.*, 16, 252
 Kneiske, T. M., Bretz, T., Mannheim, K., & Hartmann, D. H. 2004, *A&A*, 413, 807
 Mariotti, M. 2010, *ATEL*, 2510
 Mariotti, M. 2010, *ATEL*, 2684
 Mazin, D., & Raue, M. 2007, *A&A*, 471, 439
 Mattox, J. R., Bertsch, D. L., Chiang, J., et al. 1996, *ApJ*, 461, 396
 Neronov, A., & Semikoz, D. V. 2009, *Phys. Rev. D*, 80, 123012
 Neronov, A., & Vovk, Ie. 2010, *Science*, 328, 73
 Neronov, A., Semikoz, D. V., & Vovk, Ie. 2010a, *A&A*, 519, L6
 Neronov, A., Semikoz, D. V., & Vovk, Ie. 2010b, *ATEL*, 2617
 Neronov, A. N., Semikoz, D. V., Kachelriess, M., Ostapchenko, S., & Elyiv, A. 2010c, *ApJ*, 719, L130
 Neronov, A., Semikoz, D. V., & Vovk, Ie. 2010d, *ATEL*, 2610
 Stecker, F. W., Malkan, M. A., & Scully, S. T. 2006, *ApJ*, 648, 774
 Thompson, D. J., Bertsch, D. L., Dingus, B. L., et al. 1995, *ApJS*, 101, 259
 Veron-Cetty, M. P., & Veron, P. 2010, *A&A*, 518, A10